Journal of Applied Sciences and Nanotechnology, Vol. 1, No. 2 (2021)

Journal of Applied Sciences and Nanotechnology

Journal homepage: https://jasn.uotechnology.edu.iq/

Structural, Optical and Morphological Properties Cadmium Sulfide Thin Films Prepared by Hydrothermal Method

Kahlaa H. Aboud, Natheer Jamal Imran, Selma M. H. AL-Jawad*
Department of Applied Applied Sciences, Applied Physics Division, University of Technology, Baghdad – Iraq

Article information

Article history:
Received: May, 03, 2021
Accepted: June, 07, 2021
Available online: June, 25, 2021

Keywords:
CdS,
FE-SEM,
Hydrothermal method,
XRD analysis

Corresponding Author:
Selma M. H. Al-Jawad
Salma_aljawad@yahoo.com,
100069@uotechnology.edu.iq

Abstract

In this research, pure and 4%, Mn-doped thin films of cadmium sulfide (CdS) were synthesized using a 2-hour hydrothermal process. The effect of adding the dopant concentration on the samples' structural, morphological, and optical characteristics were investigated. The ultraviolet-visible-NIR spectrophotometer was used to investigate the optical properties. UV-Vis experiments lowered the optical bandgap with an add Mn percentage. Their optical bandgap was 2.38 eV for undoped thin films and 1.81 eV for 4% doped Mn-CdS thin films. UV-Vis spectroscopy data are in agreement with PL. FE-SEM imaging revealed morphological changes caused by the inclusion of Mn in CdS thin films. FE-SEM displays images of undoped CdS, which appear to be Nanoparticles. Morphology of the thin films has shown that the average grain size increases by the agglomeration of Nano-grains, which become clusters of particles after Mn^{+2}incorporation. In addition, The XRD pattern revealed that prepared samples H (002)/C (111) as hexagonal and cube phases have a preferential orientation. The increase in the main diffraction peak (002) intensity with increasing Mn concentration revealed the substitution of Mn^{+2} with Cd^{+2} in the lattice. The crystallite size increased from10.74 to 11.67 nm with an Mn percentage.

DOI: 10.53293/jasn.2021.3478.1021, Department of Applied Science, University of Technology

1. Introduction

The emergence of efficient nanostructure synthesis and characterization has opened a new frontier in the field research and advancement of novel products Due to their small size; they are often perfect crystals free of defects or internal strain. The II-VI group of nanocrystalline semiconductors is the most studied since it is relatively simple to synthesize and can often be prepared as particulates or in thin films[1]. Due to their multidimensional usefulness in a wide range of optoelectronic devices, chalcogenides are gaining a lot of interest[2]. between chalcogenide thin films such as PbS, ZnS, MnS, and CdS [3]. CdS is an important semiconductor in the II-VI group with a direct band-gap of 2.42 eV at room temperature CdS has a high degree of refraction, outstanding transport properties, and suitable energy for the photoactivation of solar electricity[4]. Moreover, simple processing processes, making CdS nanomaterials common in several fields, [3]. Two crystalline forms are presented in CdS: hexagonal phase (wurtzite) and cubic phase (zinc mixing), CdS films in both of those phases can be developed [5]. CdS possess a high affinity to the electrons and conductivity of n-type

[3]. Various methods have been used to formulate CdS thin film including chemical bath deposition [6]. Sol-gel synthesis [7], thermal evaporation [8], Electrodeposition [9], sputtering [10], metal-organic chemical vapor deposition [11], spray pyrolysis [12], hydrothermal [13], and microwave heating [14]. Each technique may produce films with a wide range of characteristics that must be tailored to a specific application. However, as previously mentioned, CdS thin films have been developed using a variety of techniques. Some of these methods are complex and/or expensive, and hydrothermal synthesis has been proved to be a relatively simple method due to its simple experimental setup and low cost [15]. CdS have a wide variety of uses in the fields of solar optoelectronics, lasers, photoconductors light-emitting diodes, Transistors, photocatalysis, and biological applications [16]. Gu et al. used a hydrothermal method to successfully synthesis an array of CdS Nanorods on $CH_3NH_3PbI_3$.surface to create a planar heterostructure solar cell with a short-circuit current up to 18.77 mA/cm^2 [17]. In this work, we have prepared pure and 4% Mn-doped CdS thin films using the hydrothermal technique. CdS and thiourea were used as precursors for pure CdS films. The Mn content in the obtained films was regulated by adding a controlled amount of Manganese sulfate with the desired weight percentage concerning CdS. The influence of Mn-content on structural, optical, and morphological properties of CdS thin film was studied in details.

2. Experimental Procedure

CdS films were deposited with hydrothermal technology on substrates. Firstly, the glass substrates were immersed in hydrochloric acid for 8 hours and then ultrasound cleaned with acetone followed by deionized water After then, it was left to dry. The details of the process of making CdS films can be found elsewhere [15]. The chemical solution that was used contains 20 ml of 0.05M cadmium sulfate ($CdSO_4.8H_2O$) salt, 20 ml of 0.1M thiourea ($CS(NH_2)_2$), and the molar concentration (4%) of $MnSO_4$ as a Dopant was dissolved in the solution. Ammonium hydroxide solution was added as a complex agent and to adjust the pH value of the solution at 12. The solutions were mixed well by stirring vigorously by using a magnetic stirrer for 15 minutes at room temperature. At last, the resulting Solution was transported into an autoclave. The autoclave was sealed into a Stainless-steel tank and maintained at 150 °C for 2 h. Then, the autoclave was left to be cooled at room temperature. The substrate has been taken out and cleaned in an ultrasonic bath using deionized water.

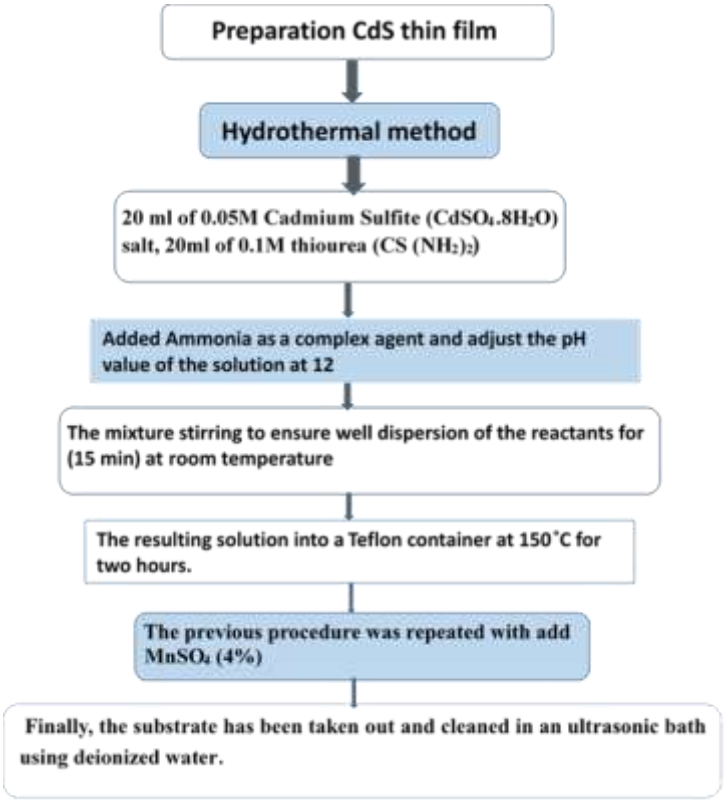

Figure1: Schematic diagrams of the preparation of CdS thin films a procedure of pure CdS, and procedure of doped CdS.

3. Characterizations

The crystal composition of the prepared CdS and 4%Mn-doped-CdS was determined by X-Ray diffraction analysis using XRD apparatus type (XRD-6000, Shimadzu, Japan) with Cu Kα radiation (λ=1.54056 Å) The measurement was set at 2θ in a range of 20° to 80°. A UV-1800 spectrophotometer (Shimadzu) was used to perform UV-Visible-NIR spectroscopy in the wavelength range of 200-1100 nm Photoluminescence (UV-Vis) FLUORESCENCE (Varian) SN: EL05043810 was used to study the electronic structure. The surface was analyzed using a FESEM (Zeiss Sigma 300- HV) Field Emission Scanning Electron Microscope (FE-SEM).

4. Results and Discussion

4.1. Structure Properties

The XRD spectra of undoped and 4% Mn-doped CdS thin films are displayed deposited on a glass substrate. In Figure 2, the result shows that all peaks are strong and sharp diffraction indicates that the CdS product is well crystallized. Diffraction spectra exhibit peaks of H (002) or C (111). Crystalline cadmium sulfate can be traced to the peaks of the diffraction sample H (102), C (220), H (112), H (004) / C (222), H (104), and (203). These planes are related to the CdS. The results confirm the presence of CdS thin film with hexagonal wurtzite and cubic structure of CdS, which are identical to the peaks of the standard datasheet (JCPDS No. 42-1411). The XRD peaks are broadened due to the nanocrystalline nature of particles. Nanocrystals have lesser lattice planes compared to the bulk, which contributes to the broadening of the peaks in the diffraction pattern [18]. The comparatively stronger peak along the (002) plane in CdS samples was indicated that the films were highly oriented along the c-axis. The identical result was also cited in the literature [15]. As shown in Figure 1, in contrast to the other peaks. According to the XRD measurements insert it may be concluded that the preferred orientation is the polycrystalline character of the films, which is preserved following Mn-ion implantation. The reduction in the (002), such a reduction in the peak intensity can be attributed to the replacement of cadmium ions with Manganese ions. The standard ion radius of Mn^{2+} (0.046 nm) is less than that of Cd^{2+} (0.097 nm). The replacement of cadmium with smaller volume atoms is expected to inhibit the growth in the same direction. This suggests that the incorporation of Mn ions resulted in the enhancement of the degree of polycrystallinity, i.e. increase of amorphization of the film through suppression of grain growth.

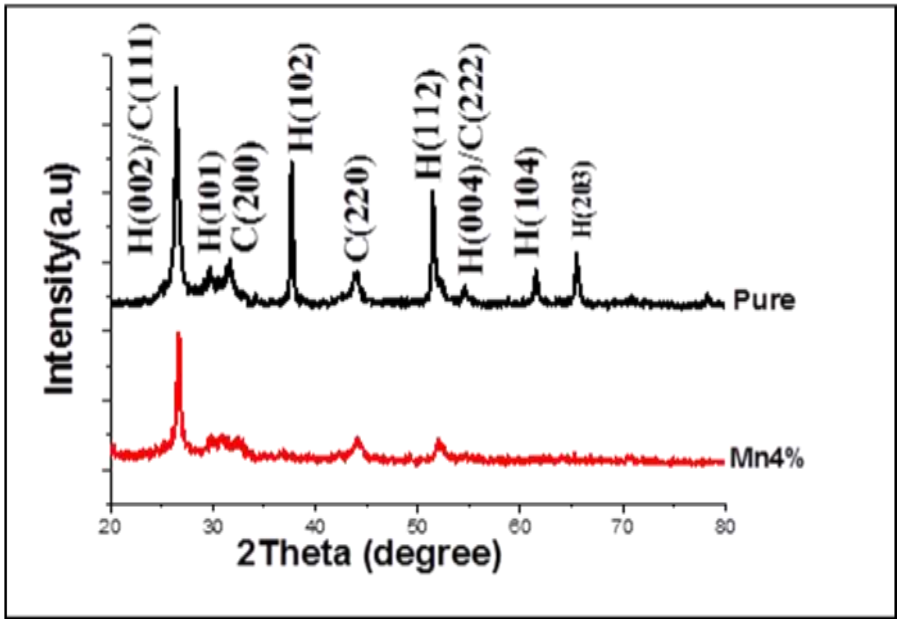

Figure 2: XRD pattern of CdS film prepared by hydrothermal method.

Table 1: Crystallite size, the position of diffraction peaks (2θ), FWHM, and lattice constants of CdS, thin films synthesized at 150 ºC for undoped and 4% Mn-doped films.

Samples	Crystal structure	D (nm)	2θ(deg.) measured	(FWHM) (deg.)	Lattice constants (Å)		
					a=b	c	c/a
pure	Hexagonal CdS	10.746	26.517	0.4228	4.17878	6.716	1.607
Mn-CdS (4) %	Hexagonal CdS	11.671	26.703	0.3887	4.142	6.669	1.61
Standard	JCPDS card no. 42-1411				4.14092	6.7198	1.6228

The crystallite size (D) of CdS was calculated from the Scherrer–Debye formula using the equation below[19], [20]:

$$G_S = \frac{A\lambda}{\Delta\theta \cos\theta} \quad \text{..... (1)}$$

Where D is the size of the particle, k is the shape factor, λ is the wavelength of X-ray (1.541 Å), β is the full-width half maximum (FWHM), and θ is the peak position. For a hexagonal-phase structure, the lattice constants a and c are calculated by the equation [21]:

$$\frac{1}{d^2} = \frac{4}{3}\left[\frac{h^2+hk+k^2}{a^2}\right] + \frac{L^2}{C^2} \quad \text{..... (2)}$$

The variation of the lattice constants with 4% doping of the manganese in CdS thin film where d, h, k, and l are Miller indicators. (Table1). The replacement of Cd ions by Mn ions due to the lower atomic size of Mn than that of Cd might be the cause of this lattice parameter shift [22].

4.2 Morphological properties

4.2.1 Field-emission scanning electron microscope

Figure 3(a&b) displays images of undoped cadmium sulfide, which appears to be nanoparticles. In our study revealed the highly dense and uniform flakes-like morphology. The particle size of CdS was about 11.27 to 91.39 nm. As seen in figure 3, this size was larger than the crystalline size of the CdS calculated by Scherrer's formula from XRD analysis. Thus, the larger particle size of CdS may be caused by Nanoplates formation. Figure 3(c&d) the irregular Nanosheets that are assembled the flower-like morphology by focusing on one of the spherical shape particles (circled by yellow color). It is clear that the obtained crystals exhibit spherical shapes with an unsmooth surface and all of them show uniform morphology. From the observation in Figure 3(c&d), those spherical shapes are a build-up of nanoparticles aggregated and formed like a flower-like structure. The change in surface morphology with adds doping Mn was attributed to the differences in the ionic radius of the ion and Cd ion. Mn^{2+} has a smaller standard ion radius [23], that each flower has a diameter of about 59.15- 227 nm.

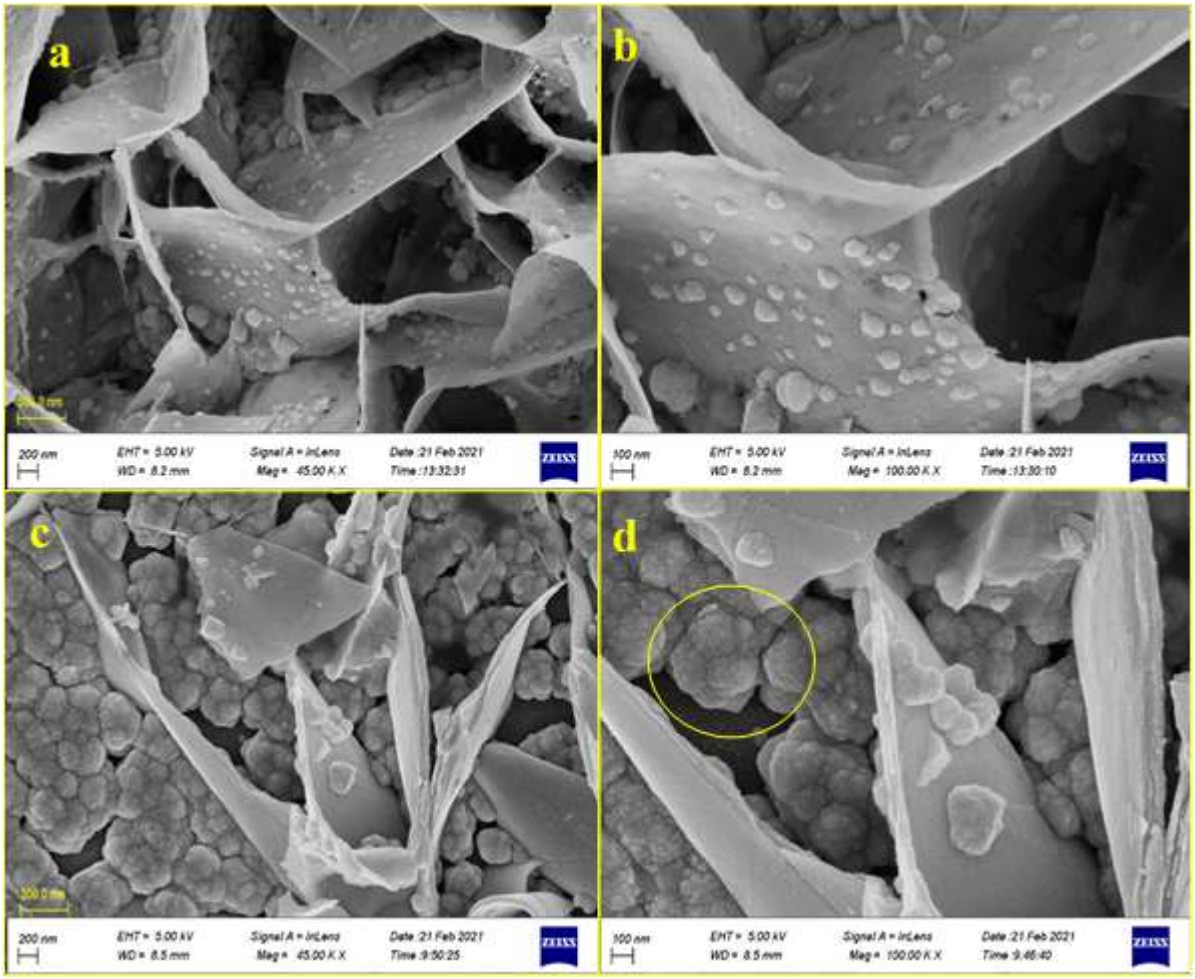

Figures 3. (a&b) represent surface FESEM of sample pure CdS and respectively **figure3** (c&d) shows the surface FESEM of sample 4%Mn doped CdS.

4.3 Optical properties

4.3.1 UV–Vis

Figure 4 shows the optical transmittance spectrum of CdS and 4 % Mn-doped CdS films. The spectrum of optical transmission depends on the material's chemical and crystal structure and film thickness and film surface structure [24]. The transmittance spectrum is characterized by the opposite behavior of the absorbance spectrum, as is shown by (Figure 4a). The transmittance spectrum is a function of the wavelength of the pure and 4% Mn-doped cadmium sulfide membranes. The optical properties of CdS thin films were investigated using a UV spectrometer across a wavelength range of 200 to 1100 nm, as shown in the visible range; these 4 percent Mn-CdS films are substantially more transparent than pure CdS films as seen. The absorption coefficient (α) was computed utilizing the formula [25]:

$$\alpha = 2.303\frac{A}{t} \quad \text{..... (3)}$$

Where t and A are respectively representatives of the film thickness and absorption.
These films' bandgaps have been determined by the equation [26], [27];

$$\alpha h\nu = Constant\left(h\nu - E_g\right)^{\frac{1}{2}} \quad \text{..... (4)}$$

Where α represents the absorption coefficient, hυ represents photon energy, and E_g represents the energy gap. The values of the band-gap were computed from the intercept of the straight-line portion of the $(\alpha h\upsilon)^2$ against hυ graph on the hυ axis as shown in Figure 4(b & c). The optical bandgap of the CdS film decreased from 2.38 eV to 1.81 eV after doping**.** Changing band gap values may be due to the influence of the different factors such as structural parameters, presence of impurities, carrier concentration, grain size, deviation from the stoichiometry of the film, and lattice strain [28].

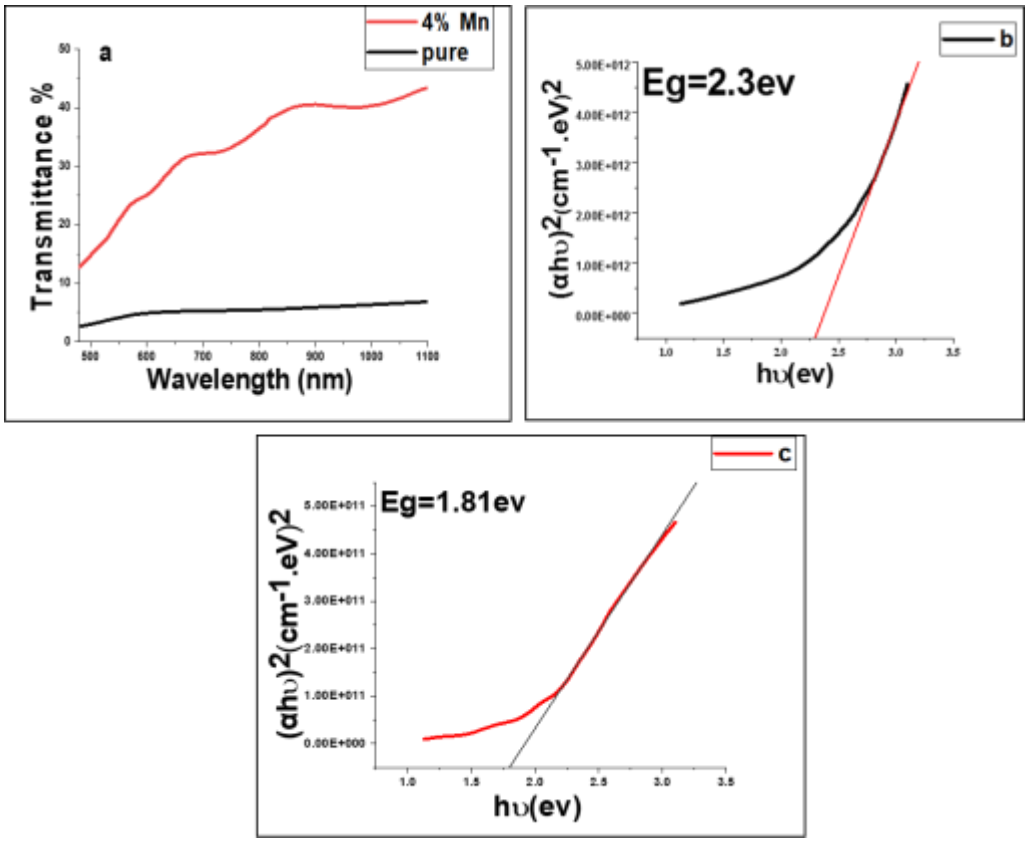

Figure 4: a) UV-Vis optical transmittance spectra **b**) energy bandgap **b)** of pure CdS and **c)** Mn-CdS 4% film.

4.3.2. Photoluminescence Spectroscopy

Figure 5 shows pristine and the 4% Mn-doped CdS thin film synthesized by the hydrothermal phase. At room temperature, the excitation wavelength is 331 nm. To observe the transition activity and to comprehend their separation and regeneration of the photogenerated carrier, PL spectroscopy was used. Deficiencies and traps in PL spectroscopy must still be investigated. The density of the trap states, on the other hand, is strongly influenced by the deposition parameters and, as a result, the system's temperature [29]. The band distance and density variations are mirrored in the trapping level. This result is in agreement with the UV-Vis results seen in Figure 4. The pure CdS band edge peak of 520 nm (2.3 eV) reveals spectroscopy changing. This is the same as the optical band gap in the transmission spectrum optical band difference. The emission ranges of the 4% Mn-doped CdS at 567 nm (2.1 eV) are almost identical to the transitional values for VB-CB. The thin film analysis at PL room temperature demonstrates this. The uniform distribution of cadmium and sulfur atoms, as well as the thermal energy associated with it, causes the shape to broaden.

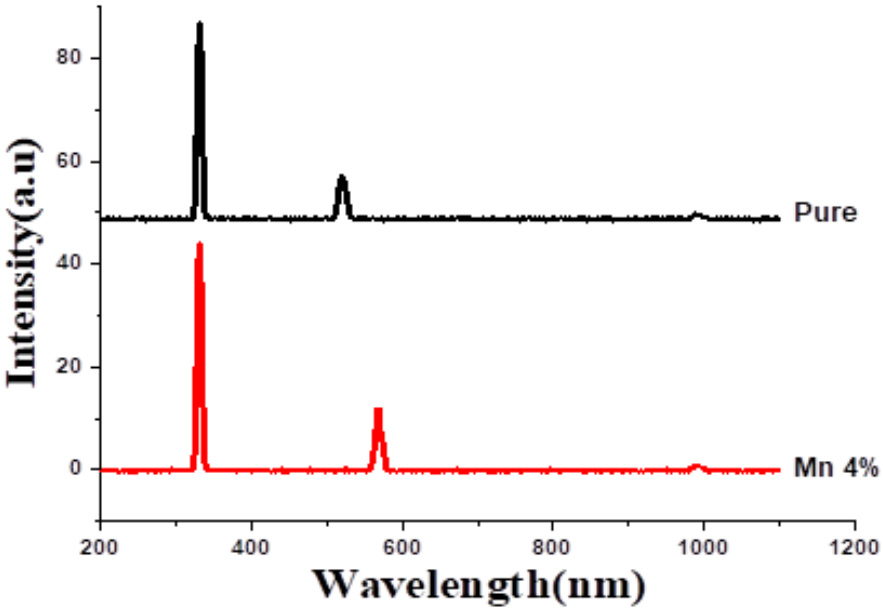

Figure 5: Photoluminescence spectra for the Pure CdS and doped CdS by Mn 4%.

5. Conclusions

CdS thin films were successfully deposited on a glass substrate at 150 ºC for 2 hours using a hydrothermal technique, which is a simple, economic, and easy method. 4% Mn-doped CdS thin film was also prepared and characterized. The adding of the Mn-doped concentration leads to an increase in the crystallite size. The film's structural, optical, and morphological properties were investigated. The polycrystalline structure of CdS samples is shown by XRD analysis. Furthermore, the crystalline size of Mn-CdS is 11.67 nm and pure 10.7 nm. The presence of sharp and high-intensity peaks in the doped material's spectrum means that it is crystalline. In addition, UV–Vis spectrum measurements show that the energy bandgap of the CdS thin film is in the range of (2.3–1.81) eV and these results are consistent with those of a photoluminescence study. The Nanoplates were discovered to be well ordered and oriented to form a flower-like assembling from the Nano flake. This image was revealed by using FE-SEM to study the morphology of the samples.

Conflict of Interest

The authors declare that they have no conflict of interest.

References

[1] Ali M. Mousa, Adawiya Jamah Haider, and Selma M.Hassan Al-Jawad, “Optical Properties of Nanostructure in CdS at Different Condition Bath Deposition,” *J. Mater. Sci. Eng. A* vol. 1, , pp. 184–190, 2011.

[2] F. Iacono, M. Purica, E. Budianu, P. Prepelita, and D. Macovei, “Structural studies on some doped CdS thin films deposited by thermal evaporation,” *Thin Solid Films*, vol. 515, pp. 6080–6084, 2007.

[3] A. Rmili, F. Ouachtari, A. Bouaoud et al., “Structural, optical and electrical properties of Ni-doped CdS thin films prepared by spray pyrolysis,” *J. Alloys Compd.*, vol. 557, pp. 53–59, 2013.

[4] Y. C. Liang and T. W. Lung, “Growth of Hydrothermally Derived CdS-Based Nanostructures with Various Crystal Features and Photoactivated Properties,” N*anoscale Res. Lett.*, vol. 11, , 2016.

[5] X. Yang, B. Wang, Y. Mu, M. Zheng, and Y. Wang, "Photocatalytic Performance of Cubic and Hexagonal Phase CdS Synthesized via Different Cd Sources," *Journal of Electronic Materials*, vol. 48, pp. 2895-2901, 2019.

[6] A. J. Khimani, S. H. Chaki, T. J. Malek, J. P. Tailor, S. M. Chauhan, and M. P. Deshpande, "Cadmium sulphide (CdS) thin films deposited by chemical bath deposition (CBD) and dip coating techniques—a comparative study," *Materials Research Express*, vol. 5, p. 036406, 2018.

[7] M. A. M. Khan, S. Kumar, A. N. Alhazaa, and M. A. Al-Gawati, "Modifications in structural, morphological, optical and photocatalytic properties of ZnO:Mn nanoparticles by sol-gel protocol," *Materials Science in Semiconductor Processing*, vol. 87, pp. 134-141, 2018.

[8] J. Trajić, M. Gilić, N. Romčević et al., "Raman spectroscopy of optical properties in cds thin films," *Sci. Sinter.*, vol. 47, , pp. 145–152, 2015.

[9] A. Zyoud, I. Saa'Deddin, S. Khudruj et al., "CdS/FTO thin film electrodes deposited by chemical bath deposition and by electrochemical deposition: A comparative assessment of photo-electrochemical characteristics," *Solid State Sci.*, vol. 18, pp. 83–90, 2013.

[10] M. A. Islam, F. Haque, K. S. Rahman, N. Dhar, M. S. Hossain, Y. Sulaiman, et al., "Effect of oxidation on structural, optical and electrical properties of CdS thin films grown by sputtering," *Optik*, vol. 126, pp. 3177-3180, 2015.

[11] I. R. C. Urbiola, J. A. B. Martínez, J. H. Borja, C. E. P. García, R. R. Bon, and Y. V. Vorobiev, "Combined CBD-CVD technique for preparation of II-VI semiconductor films for solar cells," *Energy Procedia*, vol. 57, pp. 24–31, 2014.

[12] R. Murugesan, S. Sivakumar, K. Karthik, P. Anandan, and M. Haris, "Effect of Mg/Co on the properties of CdS thin films deposited by spray pyrolysis technique," *Curr. Appl. Phys.*, vol. 19, , pp. 1136–1144, 2019.

[13] N. Loudhaief, H. Labiadh, E. Hannachi, M. Zouaoui, and M. Ben Salem, "Synthesis of CdS Nanoparticles by Hydrothermal Method and Their Effects on the Electrical Properties of Bi-based Superconductors," *J. Supercond. Nov. Magn.*, vol. 31, pp. 2305–2312, 2018.

[14] M. Husham, Z. Hassan, M. A. Mahdi, A. M. Selman, and N. M. Ahmed, "Fabrication and characterization of nanocrystalline CdS thin film-based optical sensor grown via microwave-assisted chemical bath deposition," *Superlattices Microstruct.*, vol. 67, pp. 8–16, 2014.

[15] H. K. Judran, N. A. Yousif, and S. M. H. AL-Jawad, "Preparation and characterization of CdS prepared by hydrothermal method," *J. Sol-Gel Sci. Technol.*, vol. 97, pp. 48–62, 2021.

[16] N. Shanmugam, T. Sathya, G. Viruthagiri, C. Kalyanasundaram, R. Gobi, and S. Ragupathy, "Photocatalytic degradation of brilliant green using undoped and Zn doped SnO_2 nanoparticles under sunlight irradiation," *Appl. Surf. Sci.*, vol. 360, pp. 283–290, 2016.

[17] Z. Gu, F.Chen, X. Zhang et al., "Novel planar heterostructure perovskite solar cells with CdS nanorods array as electron transport layer," Sol. *Energy Mater. Sol. Cells*, vol. 140, pp. 396–404, 2015.

[18] L. S. Devi, K. N. Devi, B. I. Sharma, and H. N. Sarma, "Influence of Mn doping on structural and optical properties of CdS nanoparticles," *Indian J. Phys.*, vol. 88, pp. 477–482, 2014.

[19] N. N. Hussein and M. M. Khadum, "Evaluation of the Biosynthesized Silver Nanoparticles Effects on Biofilm Formation," *J. applied Science and nanotechnology*, vol. 1, pp. 23–31, 2021.

[20] S. M. H. Al-Jawad, M. M. Ismail, and S. F. Ghazi, "Characteristics of Ni-doped TiO_2 nanorod array films," *J. Aust. Ceram. Soc.*, vol. 57, pp. 295–304, 2021.

[21] S. M. H. AL-Jawad, A. A. Taha, and A. M. Redha, "Studying the structural, morphological, and optical properties of CuS:Ni nanostructure prepared by a hydrothermal method for biological activity," *J. Sol-Gel Sci. Technol.*, vol. 91, pp. 310–323, 2019.

[22] S. Aksu et al., "Structural, optical and magnetic properties of Mn diffusion-doped CdS thin films prepared by vacuum evaporation," *Mater. Chem. Phys.*, vol. 130, pp. 340–345, 2011.

[23] Z. Suo, J. Dai, S. Gao, and H. Gao, "Effect of transition metals (Sc, Ti, V, Cr and Mn) doping on electronic structure and optical properties of CdS," *Results in Physics*, vol. 17, p. 103058, 2020.

[24] Adawiya Jamah Haider, Ali M. Mousa, and Selma M.H. Al-Jawad, "Annealing effect on structural, electrical and optical properties of CdS films prepared by CBD method," *J. Semicond. Technol. Sci.*, vol. 8, 2008.

[25] S. M. H. Al-Jawad, O. N. Salman, and N. A. Yousif, "Influence of titanium tetrachloride concentration and multiple growth cycles of TiO_2 nanorod on photoanode performance in dye sensitized solar cell," *Photonics Nanostructures - Fundam. Appl.*, vol. 31, pp. 81–88, 2018.

[26] S. M. H. Al-Jawad, N. J. Imran, and M. R. Mohammad, "Effect of electrolyte solution and deposition methods on TiO_2/CdS core-shell nanotube arrays for photoelectrocatalytic application," *EPJ Appl. Phys.*,

vol. 92, 2020.

[27] S. M. H. Al-Jawad, "Influence of multilayer deposition on characteristics of nanocrystalline SnO2 thin films produce by sol-gel technique for gas sensor application," *Optik.*, vol. 146, pp. 17–26, 2017.

[28] L. Wang, L. Meng, V. Teixeira, S. Song, Z. Xu, and X. Xu, "Structure and optical properties of ZnO:V thin films with different doping concentrations," *Thin Solid Films*, vol. 517, pp. 3721–3725, 2009.

[29] D. Bhattacharyya, S. Chaudhuri, and A. K. Pal, "Electrical conduction at low temperatures in polycrystalline CdTe and ZnTe films," *Mater. Chem. Phys.*, vol. 40, pp. 44–49, 1995.